Nuclear Inst. and Methods in Physics Research, A 877 (2018) 1–8

Contents lists available at ScienceDirect

Nuclear Inst. and Methods in Physics Research, A

journal homepage: www.elsevier.com/locate/nima

Measurement of exposure buildup factors: The influence of scattered photons on gamma-ray attenuation coefficients

Kulwinder Singh Mann

Department of Physics, D.A.V. College, Bathinda-151001, Punjab, India

ARTICLE INFO

Keywords:
Exposure buildup factor
Gamma-ray measurement
Optimum optical thickness

ABSTRACT

Scattered photon's influence on measured values of attenuation coefficients (μ_m, cm^2g^{-1}) for six low-Z (effective atomic number) building materials, at three photon energies has been estimated. Narrow-beam transmission geometry has been used for the measurements. Samples of commonly used engineering materials (Cements, Clay, Lime-Stone, Plaster of Paris) have been selected for the present study. Standard radioactive sources Cs^{137} and Co^{60} have been used for obtaining γ-ray energies 661.66, 1173.24 and 1332.50 keV. The optical thickness (OT) of 0.5 mfp (mean free path) has been found the optimum optical thickness (OOT) for μ_m-measurement in the selected energy range (661.66–1332.50 keV). The aim of this investigation is to provide neglected information regarding subsistence of scattered photons in narrow beam geometry measurements for low-Z materials. The measurements have been performed for a wide range of sample-thickness (2–26 cm) such that their OT varies between 0.2–3.5 mfp in selected energy range. A computer program (GRIC2-toolkit) has been used for various theoretical computations required in this investigation. It has been concluded that in selected energy-range, good accuracy in μ_m-measurement of low-Z materials can be achieved by keeping their sample's OT below 0.5 mfp. The exposure buildup factors have been measured with the help of mathematical-model developed in this investigation.

1. Introduction

Experimental measurement of γ-ray attenuation coefficient (μ_m, cm^2g^{-1}) with accuracy requires perfect narrow-beam transmission-geometry. The μ_m is the most important parameter used in non-destructive analysis of materials and CT-scan [1]. The high accuracy in measurements of the attenuation coefficients is advantageous. Practical γ-ray transmission-geometries used for such measurements usually deviate from the perfectly-narrow (good) geometry. The major cause of such deviation may be the intermixing of scattered photons with the traversing beam of photons. Such variations in the value of attenuation coefficients have been mentioned in the literature [2–4]. These researchers have concluded that for accuracy in measurements of μ_m, the sample's thickness up to 1 mfp can be used. Varier et al., [5] have been reported an opposite trend. But, they have not explained the exact cause of such type of trend. Moreover, the study was restricted to high-Z materials, e.g. Fe, Cu, Hg, Pb, etc. The maximum value of optical thickness (OT) of a sample placed in narrow-beam transmission-geometry, which can be used for accurate μ_m measurement, is termed as optimum-optical thickness (OOT). The OOT represents an uppermost value of OT for sample material up to which the influence of scattered photons can be neglected during its μ_m-measurements. In other words, the sample's thickness up to its OOT can be used for accurate μ_m measurement. The μ_m measurements for materials with higher-Z such as Hg, Pb etc., the OT value of 1 mfp can be treated as OOT for high-Z materials [5]. It has been concluded [4,6] that scattering intensity increases with the increase in sample thickness. Further, they have pointed out that for better understanding of the scattered photon's influence on μ_m measurement more experimental data is required for various scattering materials at different photon energies. Also, the increasing contribution of the incoherent scattering with an increase in sample-thickness and collimator size has been reported [3]. To the best of our knowledge information regarding OOT for low-Z (effective atomic number) materials (i.e. $Z < 20$) is missing in the literature so far.

In 1950, Gladys White observed that for a point-isotropic γ-ray source (Co^{60}) placed in a sphere of water, the experimentally measured γ-ray intensity at an appreciable distance from the source was greater than the theoretical expected intensity evaluated using total mass attenuation coefficient of water under narrow-beam

E-mail addresses: ksmann6268@gmail.com, kulwindermann@hotmail.com.

https://doi.org/10.1016/j.nima.2017.08.047
Received 8 May 2017; Received in revised form 20 August 2017; Accepted 28 August 2017
Available online 25 September 2017
0168-9002/

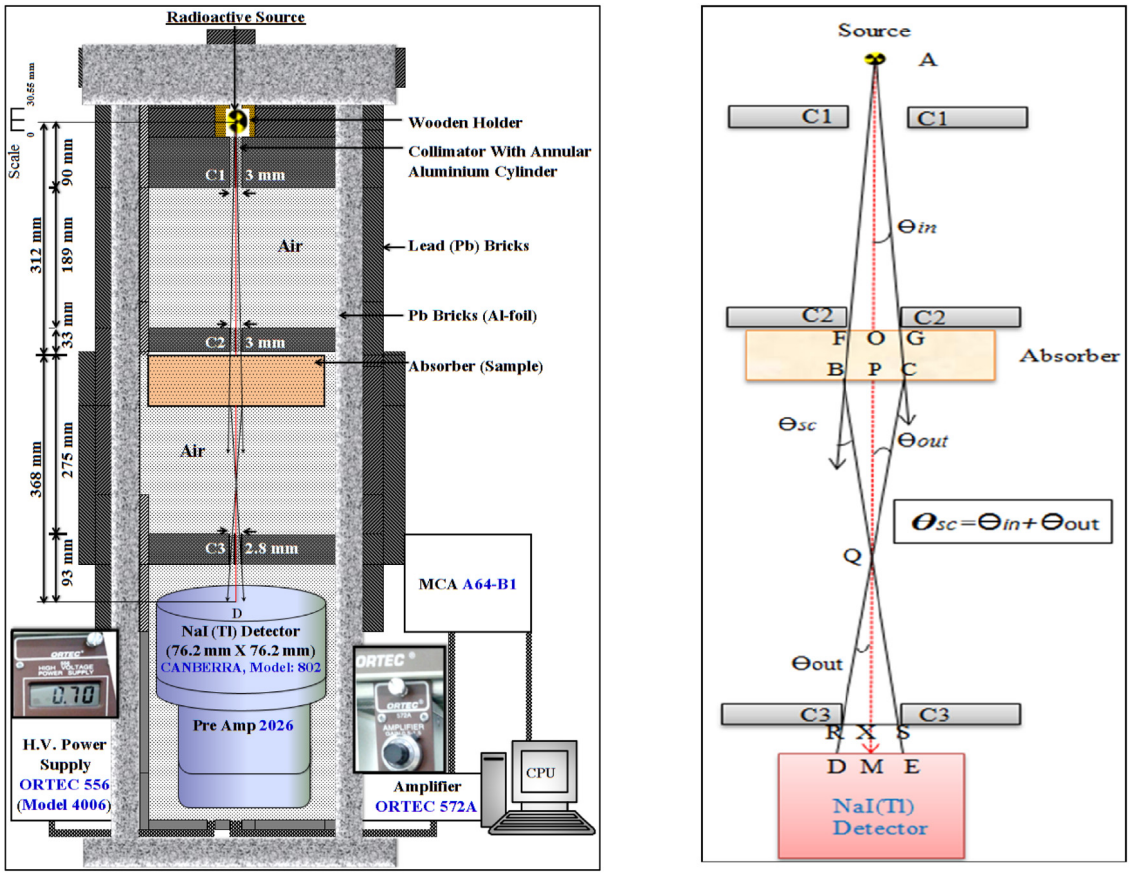

Fig. 1. Gamma-ray narrow beam transmission geometry used for the measurements [1].

conditions [7]. The underestimation in theoretical results was apparently due to neglecting the contributions of scattered and secondary radiations in theoretical computations. Thus, White introduced a new quantity, called buildup factor (B), which is defined as the ratio of measured to the computed intensity from the uncollided γ-ray photons neglecting multiple scattering [7]. It has been categorized as exposure-buildup-factor (EBF) and energy-absorption-buildup-factor (EABF) [3]. This investigation has been focussed on EBF.

In this work, the influence of scattered photons on accuracy of μ_m-measurements has been investigated for various low-Z samples at different sample-thicknesses. This work has been completed by taking various measurements for each selected sample at various (13) thickness values (ranging from 2 to 26 cm), with the help of similar experimental setup for three γ-ray energies. Thereby, the influence of scattered γ-rays on measured values of attenuation coefficients has been used to estimate the OOT for low-Z materials in the energy range 661.66–1332.50 keV. Further, with the help of mathematical model a new technique has been suggested to measure the EBF. EBFs for selected samples have been measured at various thicknesses (13) for different (3) photon energies.

2. Objective

The objective of the present study is twofold. Firstly is to provide missing information in the available literature so far regarding OOT value for low-Z materials. Secondly is to measure EBFs of the samples at various thicknesses for three γ-ray energies.

3. Theory

3.1. Attenuation coefficient and optical thickness

Including the contributions of secondary γ-rays, American Nuclear Society (ANS) standards [8] have provided huge data of buildup factors for many elements and compounds in the energy range 0.015–15 MeV, up to 40 mfp (mean free path). Harima suggested that B value depends on the deviations between interaction coefficients [9]. ANS-standards became free from errors caused by Legendre expression by using an accurate algorithm for computation of the Klein–Nishina cross section [9]. The mfp is an average distance that a monoenergetic photon travels between consecutive interactions in the given material [8]. Mathematically, it is equal to reciprocal of linear attenuation coefficient (μ, cm^{-1}) for the material. Lambert–Beer's law [10–12] expressed as:

$$I = I_0 e^{-\mu t} \tag{1}$$

where, I_0 represents incident intensity of γ-ray beam (without sample), I represents transmitted intensity of the beam (with sample of thickness t cm) and μ is the total linear attenuation coefficient (cm^{-1}) of the sample. The average-distance between consecutive interactions of γ-ray photons with matter measures its probability of interaction. This distance is named as mean free path (mfp). The mfp varies inversely with number-density (ρ_n) and cross-section (σ) of the material [13] for the γ-ray photon:

$$\lambda_m \propto \frac{1}{\rho_n \sigma} \tag{2}$$

Also, the mass attenuation coefficient (μ_m, cm^2 g^{-1}) has been defined as [13]:

$$\mu_m = \mu/\rho = \frac{1}{x} \ln\left[I_o/I\,(x)\right] \tag{3}$$

Table 1
Description of the selected samples.

Sr. No.	Sample's name	Symbol assigned	Density (g cm^{-3})	Source (Distributer; Location)	Reference of standard
1	Cement black	CB	1.652	Ultra Tech Cement, India	[22]
2	Cement white	CW	1.826	Ultra Tech Cement,India	[21]
3	Clay (Mix. of kaolinite and montmorillonite)	CY	1.743	Village Gill-Patti, Bathinda, Punjab (India)	[19]
4	Red mud	RM	1.855	Village Gill-Patti, Bathinda, Punjab (India)	[19]
5	Lime-stone	LS	1.072	Durga Lime Industries, Jodhpur, India	[18]
6	Plaster of Paris	PP	1.253	Trimurti Rajasthan, India	[20]

Table 2
Measured values of the elemental compositions of samples with wavelength dispersive X-ray fluorescence technique.

Element's symbol	Composition (by wt. fraction)					
	CB	CW	CY	RM	LS	PP
O	0.3906	0.3608	0.4507	0.4539	0.2919	0.4572
Na	0.0019	0.0014	0.0115	0.0117	0.0063	0.0005
Mg	0.0059	0.0141	0.0297	0.0284	0.0012	0.0039
Al	0.0635	0.0237	0.0895	0.0876	0.0050	0.0051
Si	0.1377	0.0980	0.2469	0.2544	0.0001	0.0122
P	0.0011	0.0001	0.0006	0.0006	0.0030	0.2080
S	0.0096	0.0173	0.0008	0.0006	0.0002	0.0001
Cl	0.0002	0.0012	0.0006	0.0004	0.0002	0.0023
K	0.0056	0.0062	0.0308	0.0290	0.6904	0.3069
Ca	0.3453	0.4728	0.0866	0.0826	0.0001	0.0004
Ti	0.0057	0.0014	0.0044	0.0044	0.0016	0.0001
V	0.0002	0.0002	0.0001	0.0001	0.0000	0.0033
Cr	0.0001	0.0001	0.0007	0.0008	0.0000	0.0000
Mn	0.0006	0.0001	0.0468	0.0452	0.0000	0.0000
Fe	0.0321	0.0025	0.0001	0.0001	0.0000	0.0000
Cu	0.0001	0.0000	0.0001	0.0001	0.0000	0.0000
Zn	0.0000	0.0000	0.0001	0.0001	0.0000	0.0000

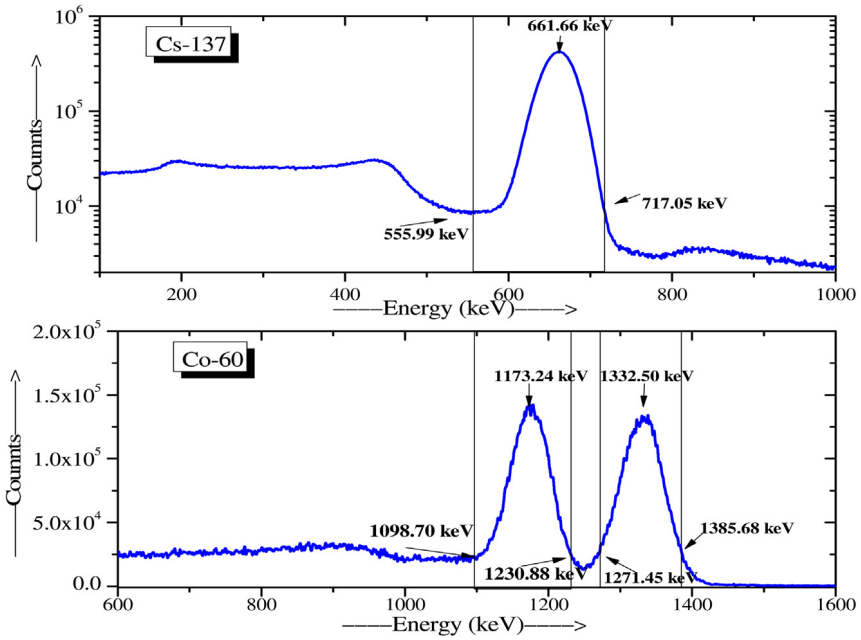

Fig. 2. Description of energy windows used for intensity measurements.

where, I (x) represents the intensity of the beam noted at a point after traversing thickness (t) of the slab-material placed between the source and the detector and x $(t \cdot \rho$, g cm^{-2}) represents areal density (mass per unit area) of the slab.

The sample-thickness, t (along the beam) in ordinary units (cm) can be converted into dimensionless-thickness, $[X = \mu \cdot t = \ln(I_o/I)]$ and termed as OT. The OT describes slab-thickness in number of mfp lengths [8]. Thus, for a slab with OT = 1 mfp, its linear thickness is $t = 1/\mu$. For the monoenergetic γ-ray, it has been found that μ-values of low-Z materials are very small as compared to high-Z materials [14–17]. Hence, for the monoenergetic γ-ray the OT of 1 mfp corresponds to a large value of the linear thickness (t) for low-Z materials as compared to high-Z materials. The ANS-standards suggest that the number of scattered photons starts increasing with the increase in material's linear thickness. Above fact indicates that for a sample-slab of 1 mfp (OT), the number of scattered photons for low-Z materials are higher than high-Z materials. This fact has been supported by ANS-standards by indicating a decreasing trend in the EBF values, with the increase in atomic-number (Z).

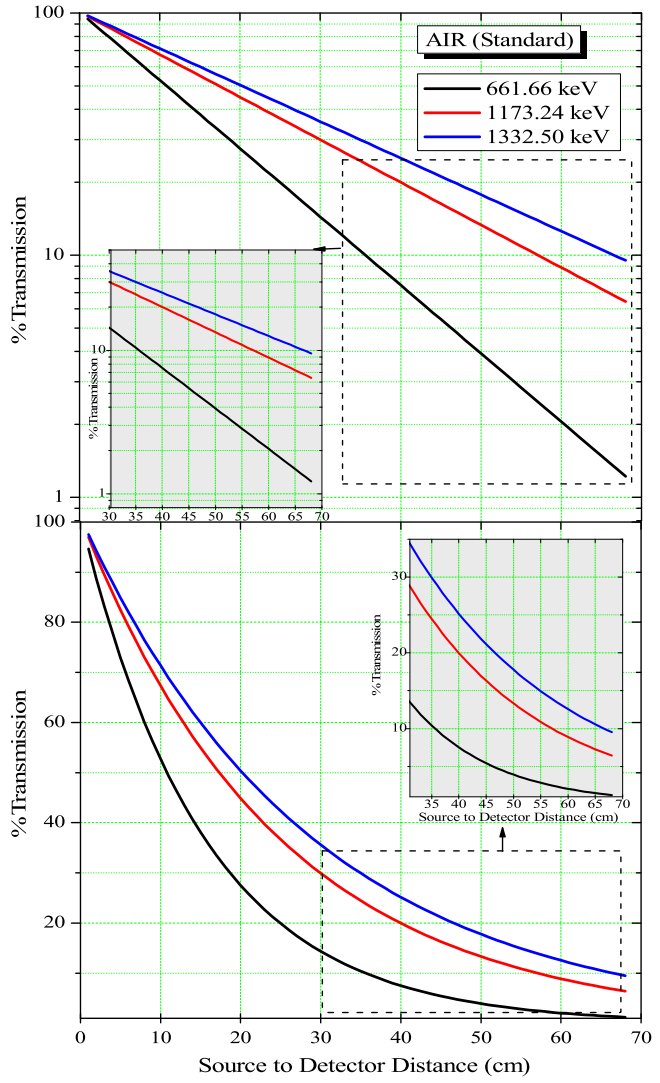

Fig. 3. Variations of gamma-ray intensities in air with source to detector distance.

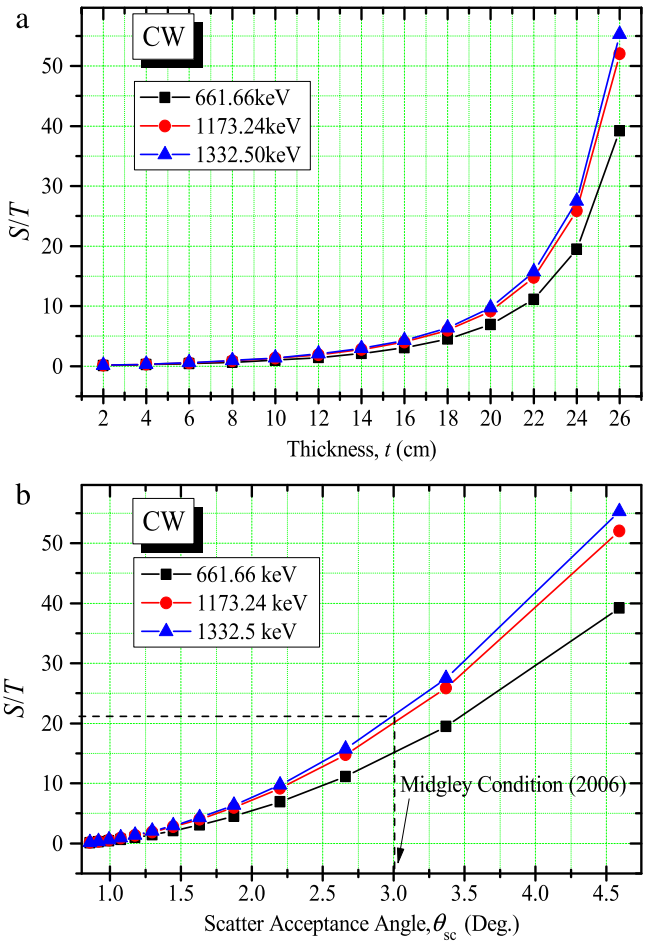

Fig. 4. Comparison between scattered to transmitted ratio (S/T) and Midgley condition [25] for narrowness of the geometry at three γ-ray energies.

3.2. Scatter acceptance angle (Θ_{sc})

Scatter-angle is defined as an angle made by the incident and scattered γ-ray photons at the outer edge of the sample (i.e. towards the detector) placed in a narrow-beam γ-ray transmission-geometry. The maximum value of the scatter-angle accepted by the detector during narrow-beam measurements is termed as the scatter acceptance angle (Θ_{sc}). This parameter is useful for verifying the narrowness of the experimental setup for measurement of γ-ray shielding parameters (GSP). As per Midgley condition [7] for the narrowness of a transmission-geometry the value of Θ_{sc} should be less than 3°.

Fig. 1 shows that $\Theta_{sc} = \Theta_{in} + \Theta_{out}$, where Θ_{in} is the angle of incidence from the point source to the sample and Θ_{out} is the angle of incidence at the point of intersection (of scattered beams) from the sample.

$$\theta_{in} = \tan^{-1}\left(\frac{\text{Effective Radius of the collimator C2}}{(\text{Source to sample distance}) + (\text{Sample's thickness})}\right) \quad (4)$$

$$\theta_{out} = \tan^{-1}\left(\frac{\text{Sum of effective Radius of the collimators C2 and C3}}{(\text{Distance between outer edges of sample and collimator C3})}\right). \quad (5)$$

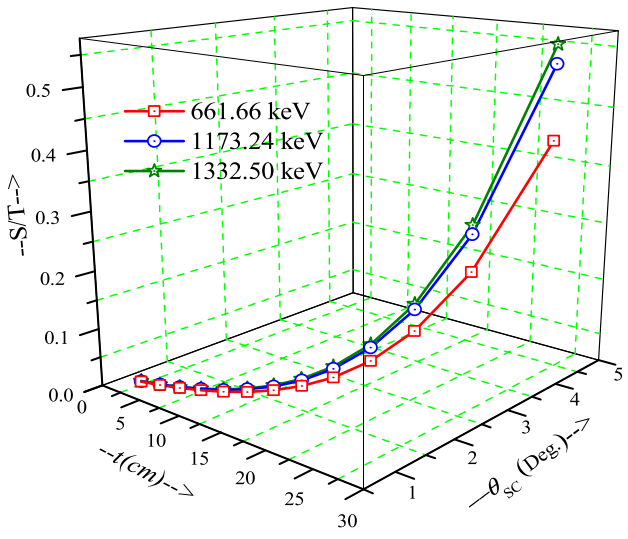

Fig. 5. Variation of S/T vs. thickness (t) and Scatter Acceptance angle (θ_{SC}) for three γ-ray photon energies.

Table 3
Description of various computed parameters for different sample-thicknesses.

t	OT = $\mu \cdot t$ (mfp)			Angle (Deg.)			S/T (No dimensions)		
(cm)	Cs^{137}, 661.66 keV	Co^{60}, 1173.24 keV	Co^{60}, 1332.50 keV	Θ_{out}	Θ_{in}	Θ_{sc}	Cs^{137}, 661.66 keV	Co^{60}, 1173.24 keV	Co^{60}, 1332.50 keV
2.00	0.28	0.21	0.20	0.58	0.28	0.86	0.11	0.14	0.15
4.00	0.57	0.43	0.40	0.64	0.28	0.92	0.24	0.32	0.34
6.00	0.85	0.64	0.60	0.72	0.28	0.99	0.42	0.56	0.60
8.00	1.14	0.86	0.80	0.80	0.28	1.08	0.66	0.88	0.93
10.00	1.42	1.07	1.01	0.90	0.28	1.18	0.99	1.31	1.40
12.00	1.70	1.29	1.21	1.02	0.28	1.30	1.44	1.92	2.04
14.00	1.99	1.50	1.41	1.17	0.28	1.45	2.09	2.78	2.95
16.00	2.27	1.72	1.61	1.36	0.28	1.63	3.05	4.05	4.30
18.00	2.55	1.93	1.81	1.60	0.28	1.87	4.52	6.00	6.37
20.00	2.84	2.15	2.01	1.92	0.28	2.20	6.92	9.19	9.75
22.00	3.12	2.36	2.21	2.39	0.28	2.66	11.15	14.80	15.72
24.00	3.41	2.58	2.41	3.09	0.28	3.37	19.49	25.89	27.49
26.00	3.69	2.79	2.62	4.32	0.28	4.59	39.20	52.05	55.28

Table 4
Measured and computed values of mass attenuation coefficients and EBFs at various thicknesses of the selected samples for three γ-ray energies.

t (cm)	Cs-137, 661.66 keV			Co-60, 1173.24 keV			Co-60, 1332.50 keV		
	μ_{exp}/ρ	μ/ρ	B	μ_{exp}/ρ	μ/ρ	B	μ_{exp}/ρ	μ/ρ	B
CB									
2	7.74E−02	7.74E−02	1.0000	5.86E−02	5.86E−02	1.0000	5.49E−02	5.49E−02	1.0000
6	7.72E−02	7.74E−02	1.0023	5.86E−02	5.86E−02	1.0001	5.49E−02	5.49E−02	1.0001
10	7.76E−02	7.74E−02	0.9975	5.85E−02	5.86E−02	1.0019	5.49E−02	5.49E−02	1.0001
14	7.51E−02	7.74E−02	1.0552	5.84E−02	5.86E−02	1.0054	5.49E−02	5.49E−02	0.9999
18	7.66E−02	7.74E−02	1.0233	5.81E−02	5.86E−02	1.0140	5.49E−02	5.49E−02	1.0003
22	7.51E−02	7.74E−02	1.0881	5.83E−02	5.86E−02	1.0129	5.49E−02	5.49E−02	1.0004
26	7.28E−02	7.74E−02	1.2208	5.83E−02	5.86E−02	1.0152	5.49E−02	5.49E−02	1.0005
CW									
2	7.77E−02	7.77E−02	1.0000	5.88E−02	5.88E−02	1.0000	5.51E−02	5.51E−02	1.0000
6	7.73E−02	7.77E−02	1.0043	5.88E−02	5.88E−02	1.0001	5.51E−02	5.51E−02	1.0001
10	7.79E−02	7.77E−02	0.9972	5.87E−02	5.88E−02	1.0022	5.51E−02	5.51E−02	1.0001
14	7.54E−02	7.77E−02	1.0614	5.87E−02	5.88E−02	1.0030	5.51E−02	5.51E−02	0.9999
18	7.46E−02	7.77E−02	1.1076	5.87E−02	5.88E−02	1.0039	5.51E−02	5.51E−02	1.0004
22	7.38E−02	7.77E−02	1.1689	5.84E−02	5.88E−02	1.0143	5.51E−02	5.51E−02	1.0004
26	7.38E−02	7.77E−02	1.2026	5.87E−02	5.88E−02	1.0056	5.51E−02	5.51E−02	1.0005
CY									
2	7.68E−02	7.68E−02	1.0000	5.83E−02	5.83E−02	1.0000	5.47E−02	5.47E−02	1.0000
6	7.63E−02	7.68E−02	1.0048	5.83E−02	5.83E−02	1.0001	5.47E−02	5.47E−02	1.0001
10	7.70E−02	7.68E−02	0.9973	5.82E−02	5.83E−02	1.0020	5.47E−02	5.47E−02	1.0001
14	7.60E−02	7.68E−02	1.0189	5.78E−02	5.83E−02	1.0115	5.47E−02	5.47E−02	0.9999
18	7.45E−02	7.68E−02	1.0750	5.80E−02	5.83E−02	1.0110	5.47E−02	5.47E−02	1.0003
22	7.45E−02	7.68E−02	1.0924	5.80E−02	5.83E−02	1.0135	5.47E−02	5.47E−02	1.0004
26	7.53E−02	7.68E−02	1.0721	5.81E−02	5.83E−02	1.0106	5.47E−02	5.47E−02	1.0005
RM									
2	7.69E−02	7.69E−02	1.0000	5.84E−02	5.84E−02	1.0000	5.47E−02	5.47E−02	1.0000
6	7.64E−02	7.69E−02	1.0060	5.84E−02	5.84E−02	1.0001	5.47E−02	5.47E−02	1.0001
10	7.71E−02	7.69E−02	0.9972	5.83E−02	5.84E−02	1.0022	5.47E−02	5.47E−02	1.0001
14	7.15E−02	7.69E−02	1.1500	5.79E−02	5.84E−02	1.0122	5.47E−02	5.47E−02	0.9999
18	7.61E−02	7.69E−02	1.0260	5.79E−02	5.84E−02	1.0157	5.47E−02	5.47E−02	1.0004
22	7.15E−02	7.69E−02	1.2457	5.79E−02	5.84E−02	1.0193	5.47E−02	5.47E−02	1.0005
26	7.46E−02	7.69E−02	1.1177	5.82E−02	5.84E−02	1.0113	5.47E−02	5.47E−02	1.0005
LS									
2	7.80E−02	7.80E−02	1.0000	5.89E−02	5.89E−02	1.0000	5.52E−02	5.52E−02	1.0000
6	7.78E−02	7.80E−02	1.0015	5.89E−02	5.89E−02	1.0000	5.52E−02	5.52E−02	1.0000
10	7.82E−02	7.80E−02	0.9983	5.88E−02	5.89E−02	1.0013	5.52E−02	5.52E−02	1.0001
14	7.72E−02	7.80E−02	1.0118	5.84E−02	5.89E−02	1.0071	5.52E−02	5.52E−02	1.0000
18	7.49E−02	7.80E−02	1.0621	5.88E−02	5.89E−02	1.0023	5.52E−02	5.52E−02	1.0002
22	7.33E−02	7.80E−02	1.1167	5.88E−02	5.89E−02	1.0028	5.52E−02	5.52E−02	1.0004
26	7.49E−02	7.80E−02	1.0909	5.88E−02	5.89E−02	1.0033	5.52E−02	5.52E−02	1.0003
PP									
2	7.76E−02	7.76E−02	1.0000	5.88E−02	5.88E−02	1.0000	5.51E−02	5.51E−02	1.0000
6	7.74E−02	7.76E−02	1.0012	5.88E−02	5.88E−02	1.0000	5.51E−02	5.51E−02	1.0000
10	7.78E−02	7.76E−02	0.9981	5.87E−02	5.88E−02	1.0015	5.51E−02	5.51E−02	1.0001
14	7.53E−02	7.76E−02	1.0417	5.87E−02	5.88E−02	1.0021	5.51E−02	5.51E−02	1.0000
18	7.29E−02	7.76E−02	1.1107	5.83E−02	5.88E−02	1.0107	5.51E−02	5.51E−02	1.0003
22	7.45E−02	7.76E−02	1.0893	5.86E−02	5.88E−02	1.0065	5.51E−02	5.51E−02	1.0005
26	7.22E−02	7.76E−02	1.1936	5.87E−02	5.88E−02	1.0038	5.51E−02	5.51E−02	1.0004

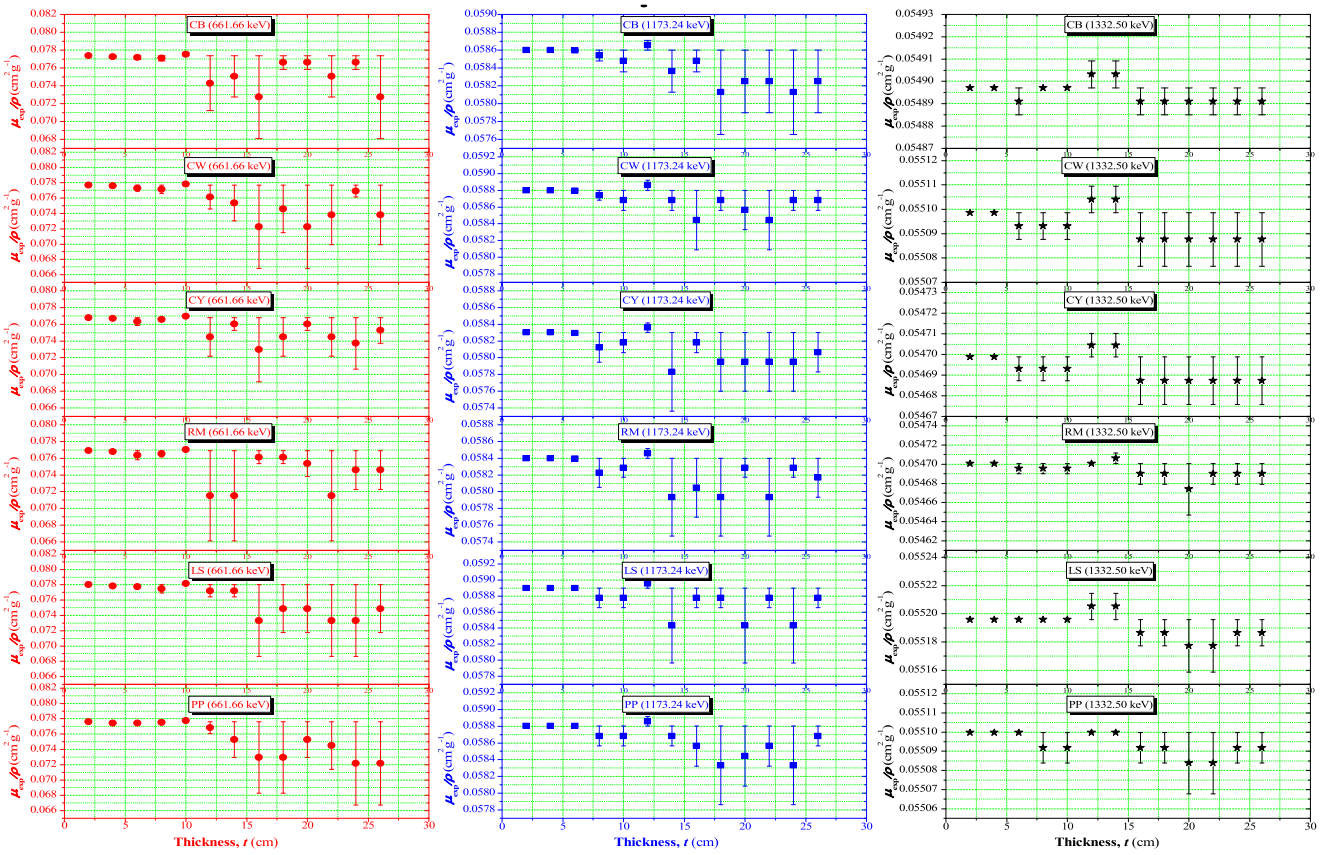

Fig. 6. Description of deviations for measured and computed values of mass attenuation coefficients for various thicknesses of selected samples at three energies.

4. Materials and methods

4.1. Sample materials

The investigation has been completed with six samples of commonly used low-Z building materials. The easy availability and reproducibility of the selected standard materials [18–22] are the reasons behind their selection. For qualitative and quantitative analysis of the sample's materials the Wavelength Dispersive X-ray Fluorescence facility has been used at Central Instrumentation Laboratory, Panjab University, Chandigarh [1]. Tables 1 and 2 provide information regarding materials and elemental compositions of the selected samples.

Three γ-rays were obtained from a point-isotropic radioactive sources, Cs^{137} (3700 MBq) and Co^{60} (370 MBq) procured from the Board of Radiation and Isotope Technology (BRIT), Bhabha Atomic Research Centre (BARC), Trombay, Mumbai, India. Gamma-ray intensities have been measured and recorded with NaI(Tl) scintillation detector (Canberra, model: 802, 2007P) coupled with MCA (2k channels, plug-in-card, ORTEC model:A64 B1) and MAESTRO computer software (Windows Model A65-B32, Version 6.01). The complete detector assembly was kept at suitable distances from all sides of laboratory viz. walls, floor, and ceiling. To protect the detector assembly from background radiations (fluorescent and scattered), the complete experimental setup was shielded with lead-alloy blocks (of thickness ≈8 cm). The lead-alloy blocks used to construct the first layer of a shield towards γ-ray beam, were wrapped in the Aluminium sheet of thickness ≈1.15 mm to minimize the production of bremsstrahlung radiations. The experimental measurements were performed in Nuclear Laboratory of the Sant Longowal Institute of Engineering and Technology, Sangrur (Punjab), India. Narrow-beam transmission geometrical setup has been adopted for the measurements using NaI(Tl) detector assembly. The stability and reproducibility of experimental setup were verified using a reference absorber (Aluminium foil, procured from Sigma-Aldrich) at 661.66 keV. To avoid any peak shifting during the experiment, various physical parameters of the laboratory were controlled by providing regulated power supply and continuously running air conditioners. During activity measurement, the magnitude of statistical errors can be reduced below 0.5% by selecting the real-time such that observed counts should be above 40,000 [23]. As suggested by Dale [23], the dead-time corrections have been applied by replacing real-time with live-time of the detector.

Theoretical computations have been performed using self-designed computer program for Gamma Ray Interaction Coefficients (GRIC2-toolkit) [1]. It is the modified form of GRIC-toolkit [24] developed by our research group. Its validation (standardized) procedure with WinXCom and GEANT4-toolkit has been published [1].

4.2. Methodology

4.2.1. Experimental setup

Two point isotropic sources (Cs^{137}, Co^{60}) and three collimators with diameters 3, 3 and 2.8 mm have been used in the investigation. Fig. 1 describes full details of the narrow-beam transmission-geometry used in this investigation. It has been proved that the geometry satisfied the narrowness condition suggested in the published literature [1,25,26].

4.2.2. Making of sample-bricks

The procedure adopted for making of bricks of samples: Firstly, a paste of the powdered sample (grain size ≤ 75μm) was prepared using distilled water. Put an appropriate amount of the paste into steel mould (95×93×50 mm) and the paste was uniformly compacted with hydraulic press (5 MPa). Freshly prepared bricks were wrapped in a polyethylene sheet and allowed to dry for 40 days in sunlight for uniform drying. The slow and uniform drying minimizes the formation of cracks due to shrinkage. The remaining moisture of each brick was removed by placing it in an oven (80 °C) for 18 h. In this way bricks of each sample have been dried safely, with minimum cracks. Thereafter, by grind the bricks for uniformity in their thickness (2 cm).

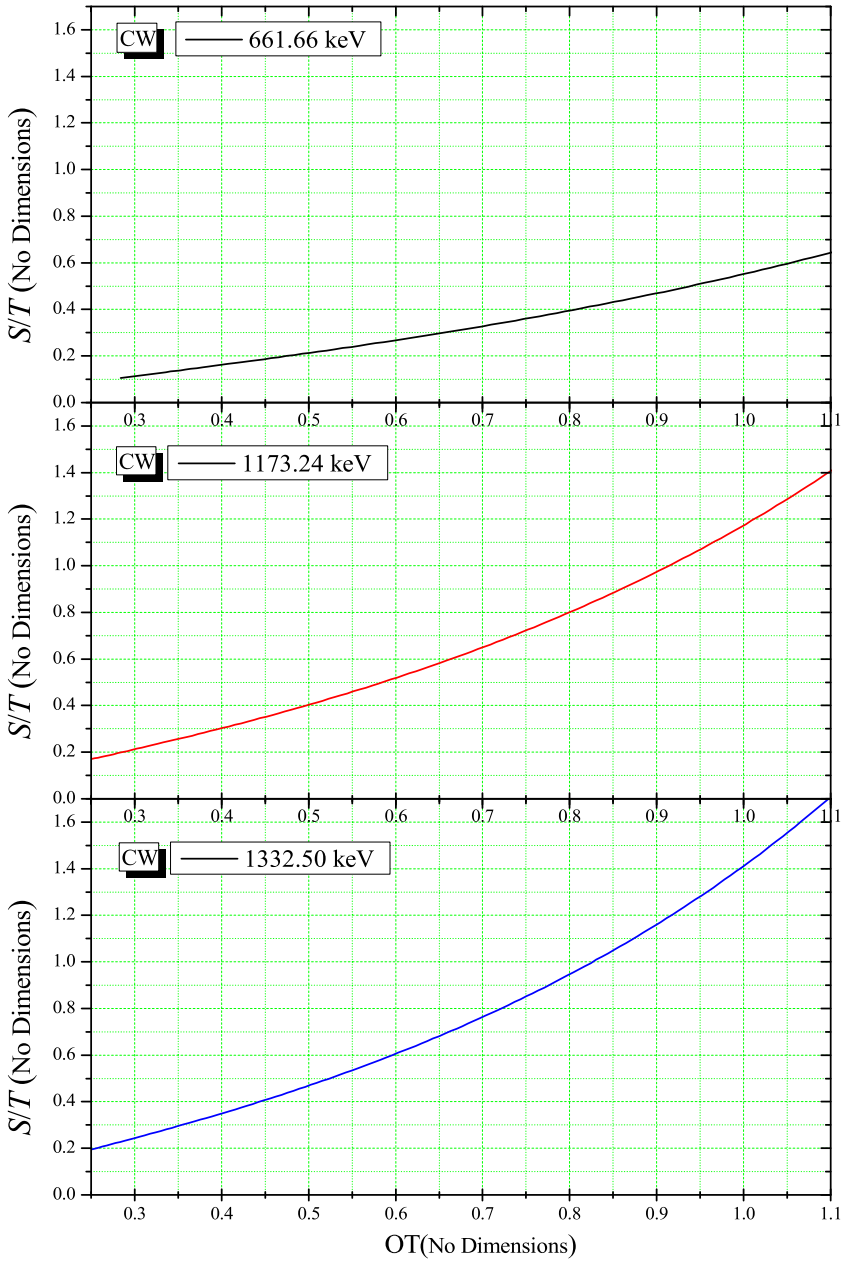

Fig. 7. Variations in scattered to transmitted ratio (S/T) with OT at three γ-ray energies for the sample (CW).

4.2.3. Measurements

Gamma-ray's photo-peak intensities without any sample (I_o) and with the sample (I) placed between the source and the detector were measured and corrected for background counts. The background counts were noted for the same real-time without placing the source in geometry. For the intensity measurements, spectrometer's dead-time correction has been applied using true counting-rate and live-time [23]. Fig. 2 describes the used energy windows for intensity measurements at selected energies. Fig. 3 explains the exponential decay of gamma-ray's intensity in the air by varying the source to detector distance. Thus, at selected energy, the μ_m values of each sample were computed by putting the recorded data in Eq. (3). The measurements for each sample and energy were repeated for at least four times. The arithmetic-mean of the computed values of μ_m has been considered as the experimental value. For fixed energy, variations of μ_m value with sample-brick thickness have been studied. Other physical parameters such as mass, dimensions and density of the samples have been measured using electronic balance of accuracy ±0.01 g, and the digital vernier calipers of accuracy ±0.02 mm.

4.2.4. Calculations

The theoretical values of μ for the samples have been computed from their elemental compositions with GRIC2-toolkit [1].

4.2.5. Mathematical model

Deviation in the measured value of μ_m with sample's thickness has been attributed to the influence of Compton-scattered-radiations. A mathematical model has been suggested to explain the cause of present observations as follows:

Though, narrow-beam geometry was established for present measurements, but perfect narrow-beam geometry can never be achieved practically. Thus, chances of scattered-radiations are always there to enter in the detector along with the transmitted beam, which accounts for the EBF (B). In such a case, the intensity of the transmitted beam

can be estimated by modified Lambert–Beer's law [27]:

$$I = B \cdot I_o \cdot e^{-\mu \cdot t}$$
$$\mu = \frac{\ln\left(I_o/I\right)}{t} + \frac{\ln\left(B\right)}{t}$$
$$\mu_{th} = \mu_{exp.} + \frac{\ln\left(B\right)}{t}$$
$$\therefore \quad B = \exp\left[\left(\mu_{th} - \mu_{exp.}\right) \cdot t\right] \tag{6}$$

where, μ_{th} represents the theoretical linear attenuation coefficient and t represents thickness of sample-brick along the beam. Since, I represents experimental transmitted intensity, the term, $\ln(I_o/I)/t$, gives the experimental value of the linear attenuation coefficient, μ_{exp}.

For practical narrow-beam geometry, ratio of scattered to transmitted (S/T) photons entering into the detector has been evaluated by the analytical-formula [28]: $S/T = N_{el,eff} \cdot t \cdot \sigma_{c,\theta sc}$. Where, $N_{el,eff}$ represents the effective electron density of the sample, $\sigma_{c,\theta sc} = \pi r_o^2 \theta_{sc}^2$ gives the Compton interaction cross-section of the photons, scattered for the θ_{sc}(scatter acceptance angle), and r_o represents the electron radius, 2.818×10^{-15} m. Fig. 4 shows that for fixed γ-ray energy by increasing sample's (CW) thickness (t or OT), the value of S/T increases thus B value increases thereby according to Eq. (6), values of μ_{exp} deviate from its theoretical value. Fig. 5 describes simultaneous variation of S/T with thickness (t) and Scatter Acceptance angle (θ_{SC}) for three γ-ray photon energies. Thus measured value of μ_m goes on decreasing with increase in sample's thickness. Thereby it has been confirmed that deviations in the measured values of attenuation coefficients for selected sample of different thicknesses may be due to intermixing of scattered photons with the transmitted γ-ray beam.

5. Results and discussion

5.1. Optimum Optical Thickness (OOT)

For the selected samples the measured values of various angles at various thickness values of the samples have been listed in the Table 3. Table 4 describes the measured and computed values of μ_m and B at three γ-ray energies at seven thickness values of the samples. Complete experimental data, for thirteen sample-thicknesses have been provided in the supplementary file. To investigate the influence of the sample's thickness and thereby scattered photons on measured values of γ-ray attenuation coefficients, the sample's thicknesses have been altered from 2 to 26 cm such that their OT varied from 0.2 to 3.5 mfp. It has been observed from Table 4 that the measured values of EBFs are higher than one (B > 1) hence provide a firm evidence for reaching of scattered photons at the detector even in the narrow beam transmission geometry.

Deviations of the measured and theoretical values of μ_m at various thicknesses of the samples have been analysed graphically. Fig. 6 shows that the variation of deviations between theoretical and measured values of μ_m at various thickness-values for each sample at three energies. The observed trend of deviations in μ_m measurement with OT (provided in the supplementary files) agreed with Varier et al., [5]. Fig. 7 explained that for fixed energy, the S/T value goes on increasing with the increase in sample's thickness, at the same time it explains that for fixed thickness, the S/T value goes on increasing with the increase in energy of γ-rays. Similar graphical descriptions of other selected samples have been provided in the supplementary files. Thus, it has been concluded that for good accuracy in μ_m measurements, low-Z sample's thickness (OT) of should remain up to 0.5 mfp. Thus, for low-Z materials, 0.5 mfp OT is termed as the OOT for μ_m-measurements in the energy-range (661.66–1332.50 keV). The OOT (0.5 mfp) for low-Z materials has been estimated by fixing the collimators size, but varying the sample's thickness. It has been concluded that OT below OOT provides good accuracy in μ_m measurement. The findings of present study show good agreement with Mika et al. [29].

6. Conclusions

It has been concluded that for low-Z materials, the μ_m-measurement with the help of γ-ray transmission-geometry, in energy-range 661.66–1332.50 keV, the optical-thickness (OT) of 0.5 mfp is considered as the optimum optical thickness (OOT).

The difference between measured and computed values of attenuation coefficients have been attributed due to the influence of scattered photons i.e. S/T and EBF. Magnitude of EBF increases with the increase in sample-thickness (t) of low-Z material which causes deviation of measured values of attenuation coefficients from their theoretically computed values.

Acknowledgements

I am grateful to Central Instrumentation Laboratory, Panjab University, Chandigarh and Nuclear Science Laboratory, SLIET, Sangrur, India for their help in this study. I am pleased for constructive comments by the esteemed reviewers.

Appendix A. Supplementary data

Supplementary material related to this article can be found online at http://dx.doi.org/10.1016/j.nima.2017.08.047.

References

[1] K.S. Mann, M.S. Heer, A. Rani, Nucl. Instrum. Methods A 797 (2015) 19.
[2] S. Gopal, B. Sanjeevaiah, Nucl. Instrum. Methods 107 (1973) 221.
[3] G.S. Sidhu, P.S. Singh, G.S. Mudahar, Radiat. Prot. Dosim. 86 (1999) 207.
[4] M. Singh, G. Singh, B.S. Sandhu, B. Singh, Appl. Radiat. Isot. 64 (2006) 373.
[5] K.M. Varier, S.N. Kunju, K. Madhusudhanan, Phys. Rev. A 33 (1986) 2378.
[6] L. Paramesh, L. Venkataramaiah, K. Gopala, H. Sanjeevaih, Nucl. Instrum. Methods 206 (1983) 327.
[7] G.R. White, Phys. Rev. 80 (2) (1950) 154.
[8] ANSI/ANS 6.4.3-1991 (W2001), American Nuclear Society, La Grange Park, Illinois.
[9] Y. Harima, Radiat. Phys. Chem. 41 (4/5) (1993) 631.
[10] P. Bouguer, Essai d'Optique sur la Gradation de la Lumi'ere, 1729.
[11] A. Beer, Ann. Phys., Lpz. 86 (1852) 78.
[12] J.H. Lambert, Germany, 1760.
[13] J.H. Hubbell, 2004, p. 7163.
[14] M.J. Berger, J.H. Hubbell, NBSIR, Vol. 87, 1987, p. 3597.
[15] J.H. Hubbell, S.M. Seltzer, NISTIR, 1995, p. 5632.
[16] D.E. Cullen, J.H. Hubbell, L. Kissel, EPDL97, UCRL-50400, 1997.
[17] M.B. Chadwick, P. Oblozinsky, M. Herman, et al., Nucl. Data Sheets 107 (2006) 2931.
[18] IS: 1128, Specification for limestone (slab and tiles) (first revision), Bureau of Indian Standards, New Delhi, India. [Reaffirmed in 2013], 1974.
[19] IS: 2720-part 40, Indian Standard Methods of Testing for Soils: Determination of Free Swell Index of Soils, BIS, New Delhi, 1977.
[20] IS: 2542-part1-12, Methods of Test for Gypsum Plaster, Concrete and Products, Part I: Plaster and Concrete, Bureau of Indian Standards, New Delhi, India, 1978.
[21] IS: 8042, Specification for white Portland cement (second revision), Bureau of Indian Standards, New Delhi, India. [Reaffirmed in 2014], 1989.
[22] IS: 3812-part1, Specification for Pulverized Fuel Ash, Part 1: For Use as Pozzolana in Cement, Cement Mortar and Concrete, 3rd revision, Bureau of Indian Standards, New Delhi, India, 2013.
[23] G. Dale, AN63, http://www.ortec-online.com/.
[24] K.S. Mann, A. Rani, M.S. Heer, Radiat. Phys. Chem. 106 (2015) 247.
[25] S. Midgley, Radiat. Phys. Chem. 75 (9) (2006) 945.
[26] B. Nordfords, Ark. Fys. 18 (1960) 37.
[27] N. Celik, U. Cevik, A. Celik, Nucl. Instrum. Methods Phys. Res. B 281 (2012) 8.
[28] C.M. Davisson, R.D. Evans, Rev. Modern Phys. 24 (1952) 79.
[29] J.F. Mika, L.J. Martin, Z. Barney, J. Phys. C18 (1985) 5215.